Mechatronics 78 (2021) 102629

Contents lists available at ScienceDirect

Mechatronics

journal homepage: www.elsevier.com/locate/mechatronics

Steering feel improvement by mathematical modeling of the Electric Power Steering system☆,☆☆

Jung Hyun Choi [a], Kanghyun Nam [b,*], Sehoon Oh [a,*]

[a] Department of Robotics Engineering, DGIST, Daegu, 42988, Republic of Korea
[b] School of Mechanical Engineering, Yeungnam University, Gyeongsan 38541, Republic of Korea

ARTICLE INFO

Keywords:
Electric steering system
Steering feel
Double Universal Joint
Torque compensation

ABSTRACT

Currently, the Electric Power Steering (EPS) system is an essential component of the vehicle because it provides assistive steering torque to the driver. To ensure a faster steering response, the position of the EPS in some vehicles is moved closer to the tire rather than the steering wheel. The steering torque, which is provided by the EPS in the steering system, mainly affects the driver's feel while steering. Therefore, the driver often feels uncomfortable owing to such positioning of the EPS in the steering system. In particular, the nonlinearity of the Universal Joint (UJ), which is one of parts of the steering system, can be felt at the steering wheel side.

In this paper, we proposed an algorithm based on the mathematical model of the steering torque in the steering system to improve the steering feel. The mathematical model is structured using parameters that can be obtained from the information of the steering system. Moreover, the formulation of the steering torque consists of the two parts, namely the deformation part, which describes the propagation inside the steering system, and the friction part that describes the inherent friction in the UJ.

Simulation and experiments were conducted to verify the proposed mathematical model with similar conditions to the real tire load during the steering motion. Furthermore, to improve the driver's feel during steering, a torque compensation algorithm is proposed and verified through experiments.

1. Introduction

The vehicle steering system performs two functions: first, it transfers the road and vehicle state information to the driver through the steering wheel, and second, it changes the driving direction. In addition to these functions, in recent years, the steering feel to the driver has become an important factor in determining the vehicle quality and the ride comfort; therefore, technologies that can improve the steering feel are required. The structure of the steering system can be divided into three parts: (1) the steering wheel, which interacts with the driver, (2) the rotating part, which includes the column, the Universal Joint (UJ), and the pinion, and (3) the rack, which includes the tie rod that is connected to the wheel. The force on the rack, which is related to the vertical vehicle load on the tires and the tire friction, is transmitted as the amount of torque on the steering wheel.

As this required steering torque is very large, a device that assists the steering torque applied by the driver was developed, which recognizes the driver's steering direction and compliments it so as to achieve the desired torque using a hydraulic device attached to either the pinion or the rack [1,2]. However, the hydraulic assistive system has several disadvantages: it requires a power device for managing hydraulic pressure, the maintenance of oil pressure is demanding, and the weight of the hydraulic device is not sufficiently light.

These drawbacks affect the efficiency of the vehicles, and thus a different type of steering assistance system called EPS (Electric Power Steering) has been developed. Nowadays, most vehicles are equipped with this device [3,4].

From the structural viewpoint, the EPS is largely categorized into two types [5]: Column type electric power steering (C-EPS) and Rack/Pinion type electric power steering (R-EPS/P-EPS). In C-EPS, the steering motor is attached to the column close to the steering wheel in a parallel way to its axis, which is widely applied in vehicles. However, the additional steering torque provided by the assistive motor may be too strong for the latter parts, and thus these parts have to be strengthened to prevent them from being twisted.

☆ This work was supported in parted by the National Research Foundation of Korea (NRF) under Grant. (NRF2019R1A2C2011444) and supported in parted by Basic Science Research Program through the National Research Foundation of Korea (NRF) funded by the Ministry of Education (2020R1A6A3A13074159).
☆☆ This paper was recommended for publication by Associate Editor Cong Wang.
* Corresponding authors.
E-mail addresses: khnam@yu.ac.kr (K. Nam), sehoon@dgist.ac.kr (S. Oh).

https://doi.org/10.1016/j.mechatronics.2021.102629
Received 4 March 2021; Received in revised form 8 May 2021; Accepted 10 July 2021
Available online 29 July 2021

In the R-EPS/P-EPS type, the steering motor is installed in parallel on either the rack side or the pinion axis. Therefore, the load on the steering devices is relatively small compared to the C-EPS type, which leads to reduction in the size of the column and the UJs. In addition, because the motor is installed closer to the wheel, it provides a faster response time of the steering than that provided by the C-EPS type. R-EPS/P-EPS is widely applied to luxury sedans owing to its advantageous steering response. In spite of these merits, R-EPS/P-EPS has the following limitations; drivers feel oscillatory behaviors even when the steering wheel is rotating at constant speeds. Moreover, unequal steering torques are detected for right and left turns around on-center steering wheel position. This phenomenon is caused by the inherent characteristic of the UJ and the position of Steering Torque Sensor (STS) in the EPS. Firstly the transformation of the rotational motion through the UJ exhibits nonlinear characteristic; in other words, the relationship between the input motion and the output motion of the UJ is nonlinear [6]. The STS of an EPS is usually installed between the steering wheel, and therefore, the relation between the STS and the steering motor differs according to the type of EPS. There exists a UJ between the STS and the steering motor in the R-EPS/P-EPS, whereas there is no STS between the UJ and the motor in the C-EPS.

In other words, the nonlinearity of the UJ affects the steering torque control in R-EPS/P-EPS. Moreover, the friction in the Revolute Joints (RJs) of the UJ is another factor which increases the nonlinearity. To overcome this undesired phenomenon, two UJs are connected in series, e.g., in the traction drive line used in trucks [7]. Nevertheless, these nonlinearities deteriorate the steering feel of the vehicle, particularly in the R-EPS/P-EPS.

The steering torque–steering angle map expression [8] has been developed and utilized as the guideline of the steering feel for EPS to realize, and many studies have focused on the precise realization of the desired steering feel described using this map, by means of EPS motor control and sensing technologies [9,10]. Other studies have been conducted focusing on the steering feel of EPS: a quantitative analysis was conducted based on measurements of the steering feel of vehicles to study the comfortable steering feel [11].

On the other hand, the nonlinearity issues of the double UJ have been studied in [12,13], but none of those studies have investigated the effect of the friction on the steering feel in a theoretical way: several studies have focused on the kinematic relationship while ignoring the friction effect inside the UJ. Even though some studies have included the friction analysis of the UJ, the results they provided are limited. For example, the mathematical analysis is missing in some studies [14], whereas in others, the results are too complicated to be applied for the actual steering system [15,16]. [17] conducted an analysis of the UJ friction and suggested a control strategy to address it, but the target EPS was only a C-EPS where the combined effect of the friction and the UJs cannot be found.

Therefore, analysis on how the frictions of the UJs appear in the steering torque in addition to the desired steering torque–angle relationship should be conducted precisely, which can be applied for the analysis of various types of EPS and the compensation of the frictions. In this study, based on the geometrical analysis of mechanical parts and sensors, we developed the mathematical model of the steering torque while taking into consideration the nonlinear characteristic of the UJ. Furthermore, based on this mathematical model, a compensation algorithm for the steering torque to improve the steering feel is proposed. The contribution points of this paper are summarized as follows:

- Mathematical formulation of the double UJ kinematics/ statics including joint frictions through the geometric approach
- Derivation of the mathematical model of steering torque as the function of pinion torque and the UJ friction considering UJ formulation
- Verification of the proposed mathematical model through precise simulations and experiments using actual UJs

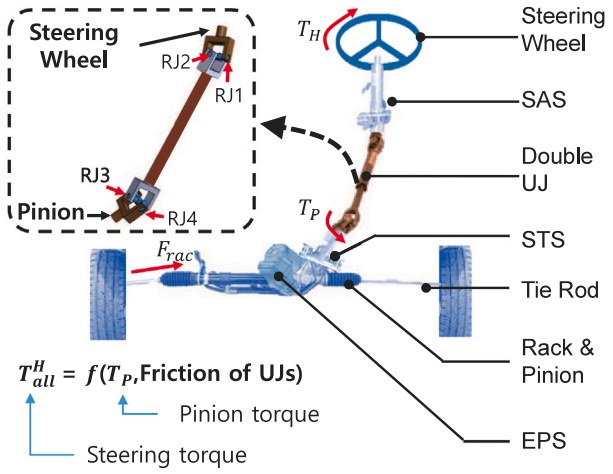

Fig. 1. An illustration of the entire steering system, which includes a double Universal Joint (UJ), the Steering Angle Sensor (SAS) and the Steering Torque Sensor (STS).

- Development of the torque compensation algorithm to achieve improved steering feel based on the proposed mathematical model

This paper is organized as follows. In Section 2 mathematical model of the steering torque is derived. Further, to verify it the simulation performed and the experimental results thus obtained are presented in Section 3. Section 4 introduces the torque compensation algorithm and the corresponding experimental results using the proposed mathematical model. Finally, Section 5 presents the conclusions of this study.

2. Mathematical model of the Double Universal Joint

In this section, we present a mathematical model of the steering system related to the steering feel. To this end, the entire steering system is analyzed to obtain the motion and torque relationship between the tire, steering wheel, and the UJs. In particular, the steering torque, which plays a dominant role in the steering feel, was investigated analytically.

2.1. Framework of the mathematical model of the steering wheel system

Fig. 1 depicts the complete structure of the Pinion type steering system, which is the focus of this study. The steering wheel is connected to the SAS (Steering Angle Sensor), which measures the steering wheel angle. The tire direction is steered through the tie rod which is driven by the rack and pinion, and the EPS is attached in parallel to the pinion axis to provide an assistive steering torque.

In particular, the STS is attached in series with the pinion axis to measure the steering torque. The assistive torque supplied by the EPS is controlled utilizing the measurement of the STS to realize the predefined impedance model that determines the steering feel.

Finally, a double-UJ connects the steering wheel and the pinion axis, thus addressing the misalignment issue. Moreover, it also transfers the steering wheel motion to the pinion as well as the contacting force of the tire to the steering wheel.

UJ is employed to efficiently transfer motion and torque between the two misaligned axes. Generally, the output motion of the UJ suffers from velocity variation due to the nonlinear characteristic of its transformation which applies even when the input motion is constant. In some applications, two UJs are connected in series to overcome this undesired distortion, e.g., in the traction drive line used in trucks [7]. However, the cancellation of the this distortion requires some special conditions to be met: the bend angles of two UJs should be the equal

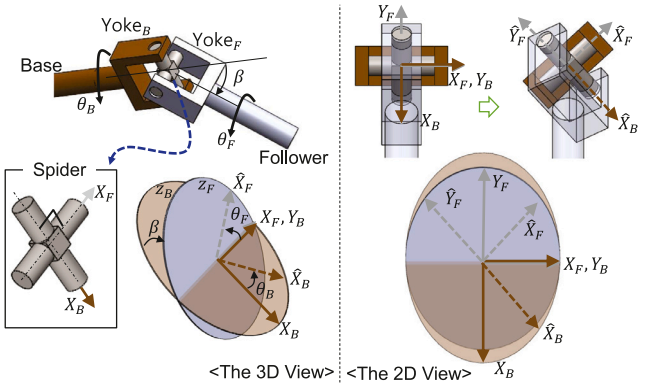

Fig. 2. Geometrical analysis of the single UJ. θ_B and θ_F are the rotation angles of the base shaft and the follower shaft, respectively. β is the bend angle or the angle of the axles with respect to each other.

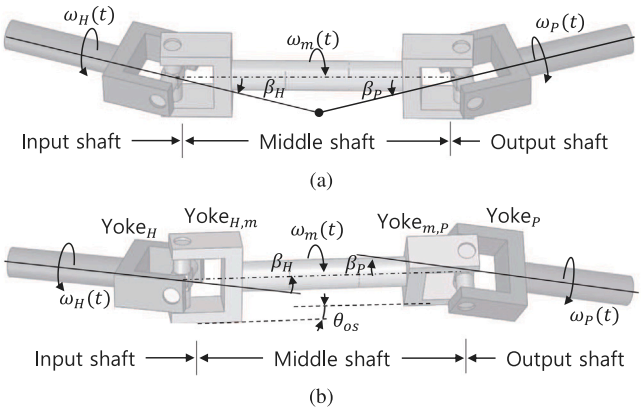

Fig. 3. Configuration of the doulble UJ (a) special configuration ($\beta_H = \beta_P$ and θ_{os}) where there is no velocity variation at the output shaft (b) general configuration which is discussed in this research.

($\beta_H = \beta_P$), and there should be no offset angle in the middle shaft ($\theta_{os} = 0$), as shown in Fig. 3(a). When these conditions are met, the condition $\omega_H = \omega_P$ holds true.

It is not always this well-conditioned double UJ that is included in the steering system. More general structure of the double UJ that is adopted in the steering system is illustrated in Fig. 3(b), where $\beta_H \neq \beta_P$, and the offset angle is non-zero ($\theta_{os} \neq 0$).

In this general configuration, velocity variation exists in the output axis; this deteriorates the steering feel. Specifically, the torque on the pinion measured by the STS is distorted at the steering wheel, which is detected by the driver. Moreover, the friction inherent in the Revolute Joints (RJs) of the UJ (as indicated at the bottom of Fig. 1) also affects the steering feel.

In this research, we mathematically investigated the torque distribution of the general double UJ. Specifically, we derived the relationship between the pinion torque T_P and the steering torque T_{all}^H, both of which are illustrated in Fig. 1.

We analyzed the steering wheel torque T_{all}^H as the summation of two terms in the RJs, namely, the transmitted pinion torque and the friction torque. These two factors should be properly converted in order to express T_{all}^H in the steering wheel axis coordinates as follows.

$$\begin{aligned} T_{all}^H(t) &= T_P^H(t) + f^H(t) \\ &= A_k T_P(t) + f^H(t), \end{aligned} \tag{1}$$

where A_k is the static relationship between the pinion torque and the steering wheel torque, which is determined by the transformation characteristic of the double UJ. $f^H(t)$ indicates the effect of the friction torque due to the RJs.

2.2. Kinematic and static analysis of double UJ through geometrical approach

To obtain A_k in (1), the kinematics of the UJ was analyzed based on the geometrical features. In a UJ, two yokes (Yoke$_B$ and Yoke$_F$ in Fig. 2) are connected via the Spider as illustrated in Fig. 2. Three dimensional relationship between two yokes can be described using the two planes of rotation Z_B and Z_F, which are perpendicular to the axis of Yoke$_B$ and Yoke$_F$, respectively.

The angle between Z_B and Z_F, which is denoted as β, determines the nonlinear transformation characteristic between θ_B and θ_F. $X_{\{B,F\}}$ and $Y_{\{B,F\}}$ denote the coordinate axes on the planes $Z_{\{B,F\}}$, respectively. As Yoke$_B$ rotates at the angle θ_B, the vector X_B rotates on the plane Z_B in the direction given by the unit vector $\hat{X}_B$. Simultaneously Yoke$_F$ rotates on the plane Z_F at an angle θ_F to $\hat{X}_B$, as shown in Fig. 2.

The equation that relates θ_B and θ_F can be expressed in terms of vectors $\hat{X}_B$ and $\hat{X}_F$ in the Z_B coordinates as follows:

$$\hat{X}_B = \left[\cos\theta_B,\ \sin\theta_B,\ 0\right], \tag{2}$$

$$\hat{X}_F = \left[-\cos\beta\sin\theta_F,\ \cos\theta_F,\ \sin\beta\sin\theta_F\right]. \tag{3}$$

It is important to note that X_B and X_F are always perpendicular because of the constraint $\hat{X}_B \cdot \hat{X}_F = 0$, which is imposed by the Spider. Therefore, θ_B can be expressed in terms of θ_F and β as follows.

$$\begin{aligned} \tan\theta_F(t) &= \frac{\tan\theta_B(t)}{\cos\beta}, \\ \theta_F(t) &= \tan^{-1}\frac{\tan\theta_B(t)}{\cos\beta}. \end{aligned} \tag{4}$$

Hence, the angular velocity of the follower in the single UJ can be obtained by differentiating (4) as follows.

$$\omega_F(t) = \frac{\cos\beta}{1-\sin^2\beta\cos^2\theta_B(t)}\omega_B(t) = A_{\theta_B}\omega_B(t) \tag{5}$$

The double UJ is composed of two UJs in series as shown in Fig. 3(a); therefore it consists of three yokes (Yoke$_H$, Yoke$_m$ and Yoke$_P$), and the relationship among their three angular velocities ω_H, ω_m, and ω_P should be analyzed. Here, β_H and β_P are the bending angles between Yoke$_H$ and Yoke$_m$ and between Yoke$_m$ and Yoke$_P$, respectively.

The middle shaft has two yokes, Yoke$_{H,m}$ and Yoke$_{m,P}$, which can be offset as shown in Fig. 3(b), where θ_{os} is the twist angle between Yoke$_{H,m}$ and Yoke$_{m,P}$. Note that Fig. 3(a) is a special configuration of the double UJ, wherein θ_{os} is set to zero, and thus two axes of Yoke$_H$ and Yoke$_P$ intersect at a certain point. In steering systems, various double UJ configurations are utilized, and therefore the general configuration of double UJ, as depicted in Fig. 3(b) should be considered with a non-zero θ_{os}.

Based on these considerations, the relationship between ω_H, ω_m, and ω_P can be expressed as follows.

$$\omega_m(t) = \frac{\cos\beta_H}{1-\sin^2\beta_H\cos^2\theta_H(t)}\omega_H(t) = A_{H,m}(t)\omega_H(t), \tag{6}$$

$$\omega_P(t) = \frac{\cos\beta_P}{1-\sin^2\beta_P\cos^2(\theta_m(t)+\theta_{os})}\omega_m(t) = A_{m,P}(t)\omega_m(t). \tag{7}$$

Finally, the resultant angular velocity relationship of the double UJ is (8) obtained by combining (6) and (7) and is given as follows:

$$\omega_P(t) = A_{m,P}(t)A_{H,m}(t)\omega_H(t). \tag{8}$$

The double UJ transmits not only the motions ω_P and ω_H but also the corresponding torques T_P and T_H, as illustrated in Fig. 4. The statics between the pinion torque T_P and the steering torque T_H can be derived

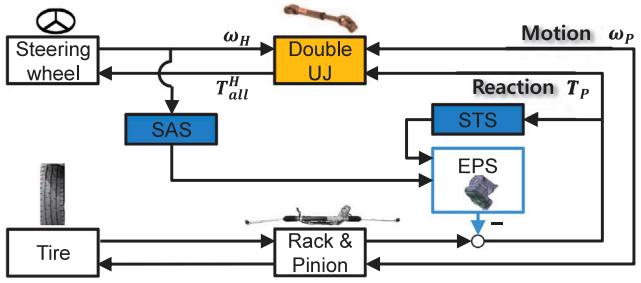

Fig. 4. Motion and torque transfer through the double UJ in the steering system.

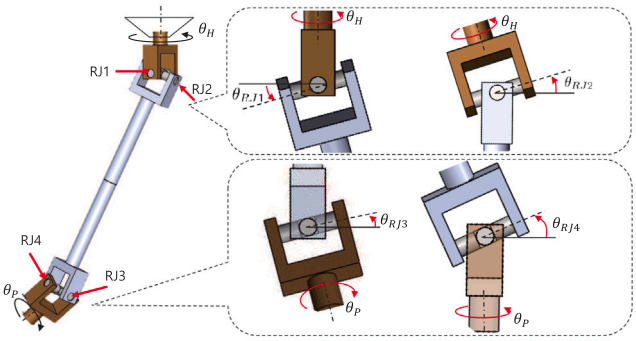

Fig. 5. Revolution Joints (RJs) in the UJ and the definition of the angle of each RJ.

based on this kinematic relationship and the virtual work principle, i.e., $T_P\omega_P - T^H_{all}\omega_H = 0$, which is given as

$$T^H_{all}(t)\omega_H(t) = T_P(t)\omega_P(t)$$
$$T_P(t) = \frac{\omega_H(t)}{\omega_P(t)}T^H_{all}(t) = A^{-1}_{m,P}(t)A^{-1}_{H,m}(t)T^H_{all}(t). \quad (9)$$

The above equation describes how the steering wheel torque T^H_{all} is transferred to the pinion, as $T_P(t)$.

Similarly the means through which the pinion torque T_P, which is generated by the interaction between the tire and the road, is transferred to the steering wheel can be derived. It should be noted that this transformation is very significant when considering the steering feel. Eq. (10) describes the steering torque T^H_P, which is transmitted from T_P.

$$T^H_P\omega_H(t) = T_P(t)\omega_P(t)$$
$$T^H_P(t) = A^{-1}_{m,H}(t)A^{-1}_{P,m}(t)T_P(t) = A_kT_P(t), \quad (10)$$

where

$$A^{-1}_{m,H}(t) = \frac{1-\sin^2\beta_H\cos^2(\theta_m(t)-\theta_{os})}{\cos\beta_H},$$
$$A^{-1}_{P,m}(t) = \frac{1-\sin^2\beta_P\cos^2\theta_P(t)}{\cos\beta_P}.$$

2.3. Friction analysis of the double universal joint

The steering feel is also effected by the inherent friction in the RJs (RJ1, RJ2, RJ3, RJ4) of the UJ. The steering feel is further complicated by the friction in each RJ, which is transmitted to the steering feel through the UJ structure. In other words, the effects of these frictions become oscillatory even if the frictions themselves are mainly of the type Coulomb friction, which is generally static in nature. Furthermore, to define this relationship, we performed a kinematic analysis to obtain the relationship of the angular velocities of RJs with respect to the steering wheel motion. Subsequently, the relationship between the friction of RJs and the steering torque is derived.

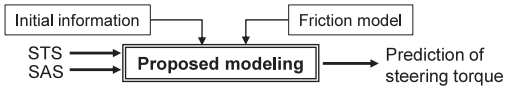

Fig. 6. The complete process required to calculate the steering wheel torque by using the sensor information and the configuration of the steering system.

Fig. 5 illustrates the angles of all the RJs namely, θ_{RJ1}, θ_{RJ2}, θ_{RJ3}, and θ_{RJ4}, which are the rotation angles along $X_{\{B,F\}}$ and $Y_{\{B,F\}}$ in Fig. 2.

Firstly, the RJ angles $\theta_{RJ\{1,2\}}$ of the first UJ are determined as

$$\theta_{RJ1}(t) = \beta_H\sin\theta_H(t), \quad (11)$$
$$\theta_{RJ2}(t) = \beta_H\cos\theta_H(t), \quad (12)$$

where, θ_H is the steering wheel angle. This relationship leads to the restriction $-\beta_H < \theta_{RJ\{1,2\}} < \beta_H$, which is implied on the RJ angles.

Following this relationship, the angular velocities of RJ1 and RJ2 are determined as follows.

$$\omega_{RJ1}(t) = \beta_H\cos\theta_H(t)\omega_H(t), \quad (13)$$
$$\omega_{RJ2}(t) = -\beta_H\sin\theta_H(t)\omega_H(t). \quad (14)$$

In this paper, the friction of ith RJ is denoted as $f_{RJi}(t)$, and Coulomb friction is assumed to be the most dominant friction at each joint. This is ascertained by the fact that the steering torque is measured when the wheel is rotated at constant speeds, and the level of the measured steering torques are almost same regardless of speeds (30, 50, 150 rpm). Therefore the friction force is expressed as $f_{RJi}(t) = -|RJi|\text{sign}(\omega_{RJi}(t))$.

The kinematic constraint of the RJs specifies the way how the frictions are reflected on the steering wheel. Hence, the virtual work principle, $f_{RJ\{1,2\}}\omega_{RJ\{1,2\}} - f^H_{RJ\{1,2\}}\omega_H = 0$ can be applied to derive the friction force transmission relationship as follows.

$$f^H_{RJ\{1,2\}}(t)\omega_H(t) = f_{RJ\{1,2\}}(t)\omega_{RJ\{1,2\}}(t),$$
$$f^H_{RJ\{1,2\}}(t) = \frac{\omega_{RJ\{1,2\}}(t)}{\omega_H(t)}f_{RJ\{1,2\}}(t). \quad (15)$$

Substituting (13) and (14) into (15) gives us the steering torque caused by the friction of RJs given as follows.

$$f^H_{RJ1}(t) = \beta_H\cos\theta_H(t)f_{RJ1}(t), \quad (16)$$
$$f^H_{RJ2}(t) = -\beta_H\sin\theta_H(t)f_{RJ2}(t). \quad (17)$$

Similar to (11) and (12), kinematics of the angular velocity of RJ3 and RJ4 can be derived as

$$\theta_{RJ3}(t) = \beta_P\sin(\theta_m(t)+\theta_{os}) = \beta_P\sin\theta_{m+os}(t) \quad (18)$$
$$\theta_{RJ4}(t) = \beta_P\cos(\theta_m(t)+\theta_{os}) = \beta_P\cos\theta_{m+os}(t) \quad (19)$$

where, θ_{m+os} is the rotation angle of $\text{Yoke}_{H,m}$ in Fig. 3(b), which consists of the rotation angle θ_m and the offset angle between $\text{Yoke}_{H,m}$ and $\text{Yoke}_{m,P}$.

By differentiating (18) and (19), the angular velocities of RJ3 and RJ4 can be represented in terms of $\omega_m(t)$ as follows.

$$\omega_{RJ3}(t) = \beta_P\cos\theta_{m+os}(t)\omega_m(t), \quad (20)$$
$$\omega_{RJ4}(t) = -\beta_P\sin\theta_{m+os}(t)\omega_m(t). \quad (21)$$

$\omega_{RJ\{3,4\}}(t)$ can also be related to the steering wheel velocity $\omega_H(t)$ by substituting (6) in (20) and (21).

$$\omega_{RJ3}(t) = \beta_P\cos\theta_{m+os}(t)A_{H,m}(t)\omega_H(t), \quad (22)$$
$$\omega_{RJ4}(t) = -\beta_P\sin\theta_{m+os}(t)A_{H,m}(t)\omega_H(t). \quad (23)$$

As for $f_{RJ\{1,2\}}$, it can be assumed the Coulomb friction mainly affects $RJ\{3,4\}$ which is represented as $f_{RJ\{3,4\}}(t) = -|RJ\{3,4\}|$

$$T^H_{all}(t) = \overbrace{A_k(t)}^{a} \cdot T_P(t) + \overbrace{\sum_{n=1}^{4} f^H_{RJn}(t)}^{b} \quad (c)$$

a. Verification of the kinematic part
- -Angular velocity comparison (Steering wheel - Pinion) (Angular velocity is not affected by the friction.)
- -Measurement of pinion angular velocity when that of the steering wheel is constant.

b. Verification of the friction part
- -Measurement of the steering torque at no load condition

c. Verification of the combined model
- -Measurement of the steering torque when subjected to various load conditions (Constant angular velocity of the steering wheel)
- -Measurement of the steering torque under the different mechanical connection conditions

Fig. 7. Verification strategy of the mathematical model.

$sign(\omega_{RJ\{3,4\}}(t))$. The amount of the frictions $f_{RJ\{3,4\}}$ transmitted on the steering wheel can be calculated utilizing the kinematic relationship derived above.

$$f^H_{RJ3}(t) = A^{-1}_{H,m}(t)\beta_P \cos\theta_{RJ3}(t) f_{RJ3}(t), \quad (24)$$

$$f^H_{RJ4}(t) = A^{-1}_{H,m}(t)\beta_P(-\sin\theta_{RJ4}(t)) f_{RJ4}(t). \quad (25)$$

Finally, the effect of all the RJ frictions on the steering wheel torque can be summarized as the summation of (16), (17), (24) and (25), as given below.

$$f^H(t) = \sum_{n=1}^{4} f^H_{RJn}(t) \quad (26)$$

2.4. Calculation of steering torque using proposed model

The complete mathematical model for the steering torque that is affected by the pinion torque given in (10) and the RJ frictions specified in (26) can be combined as shown in (27).

Based on this modeling, the T^H_{all} in (27) be estimated in real-time. Fig. 6 illustrates the estimation process, wherein $T_P(t)$ is measured using STS, and $\theta_m(t), \theta_{RJ\{1,2,3,4\}}$ can be calculated utilizing $\theta_H(t)$ measured by SAS.

θ_{os} can be calculated using $\theta_{RJ3}(0)$ in (18), which is the angle when the steering wheel is at the on-center. Moreover, β_H and β_P are the initial design parameters, which can be obtained from the manufactures.

$$\begin{aligned} T^H_{all}(t) &= T^H_P(t) + f^H(t) = A_k T_P(t) + \sum_{n=1}^{4} f^H_{RJn}(t), \\ &= \frac{1-(\sin^2\beta_H\cos^2(\theta_m(t)-\theta_{os}))}{\cos\beta_H}\frac{1-\sin^2\beta_P\cos^2\theta_P(t)}{\cos\beta_P}T_P(t) \\ &+ \beta_H\cos\theta_{RJ1}(t) f_{RJ1}(t) + (-\beta_H\sin\theta_{RJ2}(t)) f_{RJ2}(t) \\ &+ A^{-1}_{H,m}(t)\beta_P\cos\theta_{RJ3}(t) f_{RJ3}(t) \\ &+ A^{-1}_{H,m}(t)\beta_P(-\sin\theta_{RJ4}(t)) f_{RJ4}(t). \end{aligned} \quad (27)$$

3. Verification of the steering wheel torque mathematical model

In this section, the verification of the proposed steering wheel torque model in (27) through simulations and experiments is presented.

The model consists of two parts — kinematic relationship $A_k(t)$ and the friction effect $f^H(t)$. Accordingly the experimental verification is conducted in three steps, as shown in Fig. 7. Firstly, to verify the kinematic relationship in (8), the angular velocity of the pinion axis was measured with a certain steering wheel motion pattern, which was then compared with the calculation output obtained using (6), (7) and (8). Secondly, the effect of friction on the steering wheel f^H in (26) was verified through the experimental results with the pinion torque T_P set to 0. Finally, a total wheel torque was measured with loads on the pinon to mimic the rack force F_{rac} [18], and the steering torque thus measured was compared with the model results of (27), which represent the results of the proposed model.

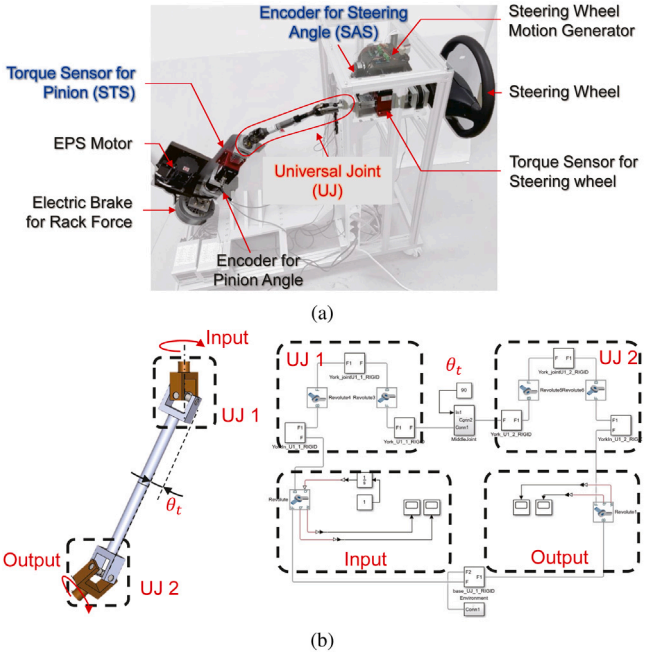

Fig. 8. Verification Environments (a) Experimental setup to verify the proposed mathematical model of the steering system (b) Simulation model based on the Simscape™in the Matlab©/Simulink© environment.

Fig. 8(a) illustrates the experimental apparatus, which consists of following components.

- Two torque sensors (STS) and encoders (SAS) for measuring the torque/angle of the pinion and the steering wheel axis.
- One variable electric brake at the pinion axis to mimic the rack force.
- One motor at the steering wheel axis to generate the rotary motion to the mimic driver's motion.
- One motor at the pinion axis to compensate for the steering wheel torque fluctuation due to nonlinearity and friction.
- A dual universal joint with various friction conditions.

Because the target system of this research was the R-EPS, a EPS motor was installed on the pinion side to provide the assistive steering torque. Moreover, in this study, this motor was also utilized to compensate for the effect of the nonlinearity of the UJ and its friction. The torque sensor STS was attached on the pinion axis, and the angle sensor SAS was attached on the steering wheel axis. The measurements of STS and SAS were utilized to calculate T^H_{all}, as illustrated in Fig. 6.

Moreover, the steering wheel axis torque sensor and the pinion axis angle sensor were added to verify the mathematical model proposed in this paper. These sensors were used only for the verification and were not utilized in the actual vehicle steering system.

Furthermore, an electric motor was installed to generate patterned steering wheel motion, and an electric brake was attached on the pinion to mimic the rack force.

Because the measurements in the experiments could not measure the details of each component, simulations were conducted to verify these details of friction obtained using the proposed model. Fig. 8(b) shows the Matlab© /Simulink© simulation environment of the steering system. The physical model of the steering system was first drawn using the 3D CAD tool and was then imported to Simulink© using Simscape™.

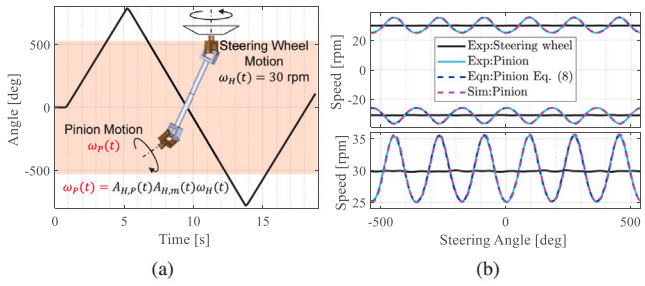

Fig. 9. Verification of the kinematic model: (a) Experimental condition of the double UJ (b) Experimental results.

3.1. Verification of kinematic model

The kinematic model, A_k, was verified by comparing the angular velocities of the pinion axis calculated from (8) and the actual experimental measurements. In the experiment, the steering wheel was rotated left and right rotate at the constant speed of 30 rpm; from the on-center to −540° then to 540° and back to the on-center, as shown in Fig. 9(a).

The results are plotted in Fig. 9(b) where the solid black, solid cyan, and dashed blue lines indicate the angular velocity of the steering wheel, the experimental results, and the equation of the pinion axis, respectively. Note that the experimental values of the steering wheel angular velocity were used for the ω_H in (8).

As expected, the oscillation of the pinion axis was observed even when the steering wheel was rotated at a constant speed. The results of the equation and the experiment were approximately equal with 0.12 Root Mean Square Error (RMSE), which verifies that the proposed kinematic model can depict the kinematic relationship satisfactorily. Moreover, the simulation model, which represents the actual UJ was verified as shown by the magenta solid line in Fig. 9(b), which is similar to the experimental result.

3.2. Verification of the friction torque model

We verified the friction effect of RJs to the steering wheel torque. First, the angular velocities of RJs with respect to the steering wheel angular velocity in (13), (14), (22) and (23) are verified. The effects of the RJ frictions on the steering wheel torques given by (16), (17), (24), and (25) were verified. The verification of the angular velocity relationship was conducted only through simulation, because it was difficult to measure the angular velocities of the RJs experimentally.

To verify the kinematics the steering wheel was rotated at a constant speed of 5 rad/s (solid black line in Fig. 10) from the on-center to 540°. All the solid lines indicate the simulation results, and all the dashed lines indicate the results of the modeling. Fig. 10(a) plots the comparison between the simulation results and the model output obtained using (13), (14), (22), and (23). The oscillatory behavior can be observed in the RJs even when the steering wheel is rotated at a constant speed. The angular velocity of each RJ is observed to be lower than the actual steering wheel speed (5 rad/s). Moreover it can be observed that velocities calculation performed using (13), (14), (22), and (23) were approximately equal to the velocities obtained from simulations. The corresponding RMSE values for these velocities were calculated as 0.23, 0.21, 0.32, and 0.33, respectively, which validates that the proposed RJ velocity model is sufficiently accurate.

Fig. 10(b) graphs the simulation results of the four different steering torques, where the steering wheel is rotated similarly to that done in the case of Fig. 10(a). The RJ friction in this simulation was considered to be Coulomb friction with an amplitude of 0.1 N s/m (solid black line).

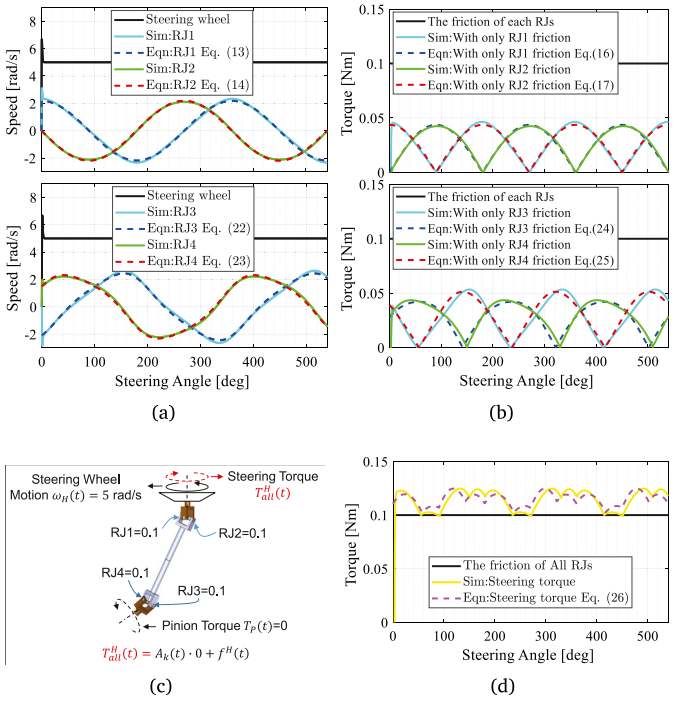

Fig. 10. Verification of RJ motion and torque through the Simcape™Model (a) Verification of the motion model between steering wheel and RJ1,RJ2,RJ3, and RJ4 (b) Verification of the friction model between steering wheel and RJ1,RJ2,RJ3, and RJ4 (c) Condition of the double UJ in the friction experiment (d) Steering torque verification of the friction using (26).

It is interesting that the magnitudes of the friction forces transmitted to the steering torque are smaller than the actual friction forces in the RJs. This phenomenon can be also verified using (16), (17), (24), and (25) between the simulation and calculation results, the calculated values of RMSEs of the steering torque were 0.002, 0.002, 0.006, and 0.007, respectively, which verifies the accuracy of the proposed model.

Finally, the steering torque by frictions in all the RJs are depicted Fig. 10(c). The simulation result obtained using this friction condition is plotted in Fig. 10(d) and is compared with the calculation results of (26). The pattern of the steering torque (solid yellow line) was observed to be periodic, and the magnitude of the summed friction is approximately equal to the calculation result.

In the experiment, various UJs with different friction of RJ were used to verify the results of (26). Specifically, for calculating the steering torque using (26), the value of friction of each RJ is required and the UJ manufacturer provides rough Coulomb friction values. Fig. 11 graphs the experimental results of the steering torque for four different UJ samples labeled as UJ#1, UJ#2, UJ#3, and UJ#4. The corresponding RMSE values obtained from experimental results and equations (dashed green line) are 0.044 N m, 0.087 N m, 0.051 N m, and 0.088 N m, respectively. Thusly, friction model of the UJ was verified.

3.3. Verification of the combined mathematical model

To verify the combined model expressed in (27), which is complete mathematical model proposed in this paper, the experimental conditions were set as illustrated in Fig. 12(a). The combined load (constant and elastic) was applied to the electric brake to ensure that it imitated the rack and pinion system in the vehicle. Note that the experimental values of the pinion torque were used for $T_P(t)$ in (27) to compare the steering torque under the same conditions. Other experimental conditions, including motion and speed of the steering wheel, are same

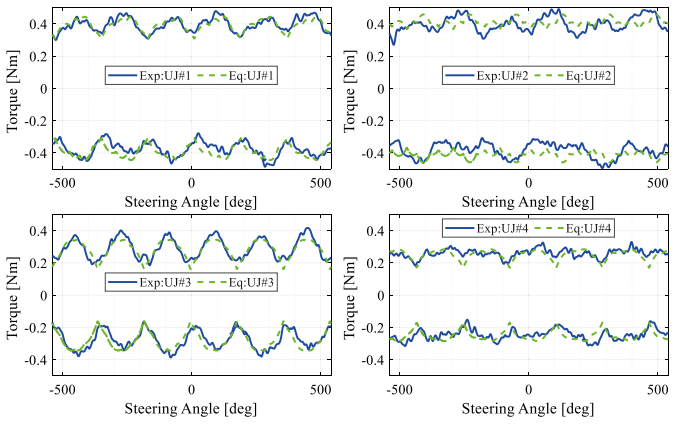

Fig. 11. Experimental results for various UJ samples with different RJ friction values. The steering wheel motion was set to 30 rpm and under no load condition at the pinion axis.

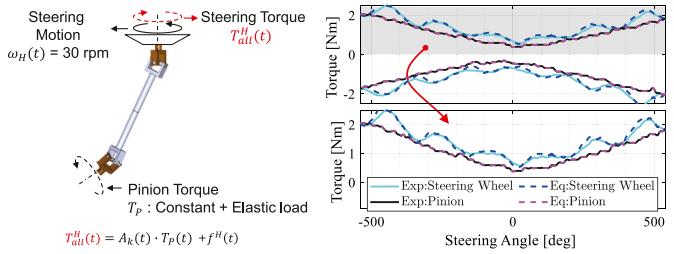

Fig. 12. Experimental results for comparison between the steering torque obtained from Eq. (27) and the experiment.(a) Experimental condition (b) Verification of the whole mathematical model of the UJ with constant and elastic load at the pinion axis. The RMS error was observed to be 0.23 N m.

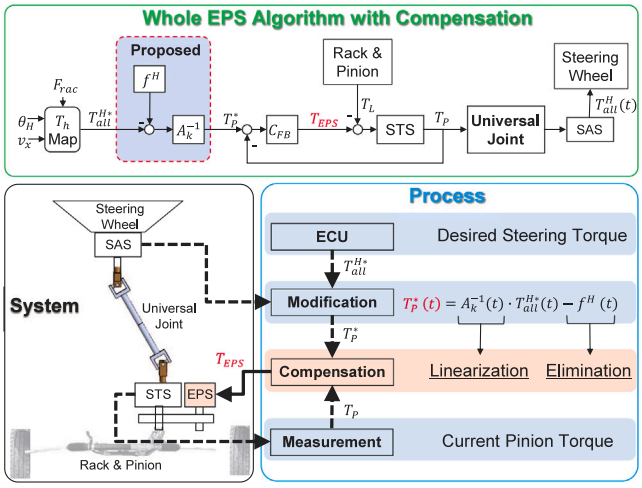

Fig. 13. The torque compensation strategy for improving the steering feel in the steering system.

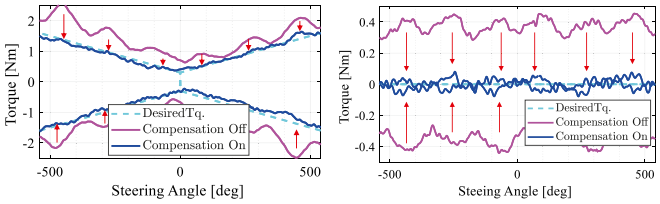

Fig. 14. Torque compensation experimental results (a) Torque compensation for linearization of the steering wheel torque (b) Torque compensation to eliminate friction inside of UJ.

as those applied in Section 3.1. Experimental results are plotted in Fig. 12(b) where solid black, solid cyan, and dashed blue lines represent measured pinion torque, measured steering torque, and the steering torque calculated using (27). The RMSE was determined to be 0.23 N m. Thusly the proposed mathematical model was verified.

4. Steering feel improvement control based on the mathematical model

4.1. Steering feel improvement by torque compensation

It can be observed from Fig. 12(b) that the steering torque is oscillatory and unbalanced at the on-center which is uncomfortable for the driver. A torque compensation algorithm that is to be run in the EPS to improve this undesired steering feel, is proposed in this paper.

Fig. 13 describes the whole torque compensation algorithm in the steering system. In the conventional EPS algorithm, T_{EPS} is calculated by using T_{all}^{H*} which is the desired steering torque, and T_{STS}, which is the measured torque at the pinion, as follows:

$$T_{EPS}(t) = C_{FB}(T_{all}^{H*}(t) - T_p(t)), \tag{28}$$

where, T_{all}^{H*} is the desired steering torque which is same as T_P^*, and is predefined through the T_H-Map basing on the vehicle states, which are described using parameters such as steering angle (θ_H), steering speed ($\dot{\theta}_H$), rack force(F_{rac}), and vehicle speed (v_x) [19].

However, as mentioned in Introduction, the steering torque T_{all}^H is different from the pinion torque T_P because of the UJ that is installed between the STS and the steering wheel. To compensate for this difference, the desired pinion torque T_P^* is modified based on the mathematical model proposed in this paper. The properties of the T_P^* are: (1) linearization of the non-linearity between the steering torque and pinion torque by using A_k^{-1}, and (2) elimination of the friction effect using f^H as follows:

$$\begin{aligned} T_P^*(t) &= A_k^{-1}(t)(T_H^*(t) - f_H(t)) \\ &= A_k^{-1}(t)T_H^*(t) - A_k^{-1}(t)f_H(t). \end{aligned} \tag{29}$$

4.2. Torque compensation experimental result

To verify the torque compensation algorithm derived in (29), an experiment was conducted with the combined load applied to the electric brake to mimic the rack and pinion condition in the vehicle. Other experimental conditions are the same as in Section 3.1. Results are plotted in Fig. 14(a) where dashed cyan, solid magenta, and solid blue lines represent the assumed desired steering torque T_{all}^{H*}, torque results obtained without compensation, and those obtained with compensation, respectively. From these results, it was observed that the oscillation phenomenon was reduced significantly due to the torque compensation; moreover, the steering torque was approximately equal to the desired one, due to which the steering feel was improved. During torque compensation, the effectiveness of friction elimination was also verified as plotted in Fig. 14(a). Because the no load condition ($T_{rac} = 0$) was applied to the electric brake in this experiment, the desired steering torque T_{all}^{H*} was also zero.

Therefore (29) can be rewritten as $T_P^*(t) = -A_k^{-1}(t)f_H(t)$. The result of friction elimination is effective as depicted in the figure using a comparison between the solid blue line and the solid magenta line.

5. Conclusion

In the steering system, the double Universal Joint (UJ) causes oscillatory and undesired torque in the steering wheel. To address this problem, we proposed a mathematical model of the steering system to improve the steering feel by compensating the oscillatory steering torque and friction.

Based on the geometrical approach of the double UJ, the equation of the double UJ was derived; it consists of two parts: (1) the kinematic part, which transfers the torque from the pinion to the steering wheel, and (2) the friction part, which describes friction of the RJs of the UJ. Moreover, the proposed mathematical model including the formulation of UJ was arranged by considering its application to the embedded system with available sensors installed in the steering system. Three different verification strategies were introduced by using a simulation model and an experimental setup. Results show that the proposed mathematical model satisfactorily describes the steering torque in various experimental conditions. Furthermore, the improvement of the steering feel achieved by implementing the proposed mathematical model was confirmed through the torque compensation experiments.

CRediT authorship contribution statement

Jung Hyun Choi: Conceptualization, Methodology, Validation, Writing – original draft, Visualization. **Kanghyun Nam:** Investigation, Formal analysis, Supervision. **Sehoon Oh:** Writing – review & editing.

Declaration of competing interest

The authors declare that they have no known competing financial interests or personal relationships that could have appeared to influence the work reported in this paper.

References

[1] Kemmetmuller W, Muller S, Kugi A. Mathematical modeling and nonlinear controller design for a novel electrohydraulic power-steering system. IEEE/ASME Trans Mechatronics 2007;12(1):85–97.

[2] Dell'Amico A, Krus P. Modeling, simulation, and experimental investigation of an electrohydraulic closed-center power steering system. IEEE/ASME Trans Mechatronics 2015;20(5):2452–62.

[3] Choi H-R, Choe G-H. A multiobjective parametric optimization for passenger-car steering actuator. IEEE Trans Ind Electron 2010;57(3):900–8.

[4] Kim W, Son YS, Chung CC. Torque-overlay-based robust steering wheel angle control of electrical power steering for a lane-keeping system of automated vehicles. IEEE Trans Veh Technol 2015;65(6):4379–92.

[5] Hur J. Characteristic analysis of interior permanent-magnet synchronous motor in electrohydraulic power steering systems. IEEE Trans Ind Electron 2008;55(6):2316–23.

[6] Seherr-Thoss H-C, Schmelz F, Aucktor E. Universal joints and driveshafts: analysis, design, applications. Springer Science & Business Media; 2006.

[7] Mazzei Jr AJ. Passage through resonance in a universal joint driveline system. J Vib Control 2011;17(5):667–77.

[8] Salaani MK, Heydinger GJ, Grygier PA. Experimental steering feel performance measures. SAE Trans 2004;665–79.

[9] Balachandran A, Gerdes JC. Designing steering feel for steer-by-wire vehicles using objective measures. IEEE/ASME Trans Mechatronics 2014;20(1):373–83.

[10] Lee MH, Ha SK, Choi JY, Yoon KS. Improvement of the steering feel of an electric power steering system by torque map modification. J Mech Sci Technol 2005;19(3):792–801.

[11] Pfeffer PE, Harrer M, Johnston D. Interaction of vehicle and steering system regarding on-centre handling. Veh Syst Dyn 2008;46(5):413–28.

[12] Petrescu FI, Petrescu RV. The structure, geometry, and kinematics of a universal joint. Indep J Manag Prod (Ijm&P) 2019;10(8).

[13] Hayama Y. Dynamic analysis of forces generated on inner parts of a double offset constant velocity universal joint (DOJ): non-friction analysis. Tech. rep., SAE Technical Paper; 2001.

[14] Sun G, Ren W, Zhang J. Virtual product development for an automotive universal joint. Int J Automot Technol 2011;12(2):299–305.

[15] Sheu P-P, Chieng W-H, Lee A-C. Modeling and analysis of the intermediate shaft between two universal joints. J Vib Acoust 1996;118(1):88–99.

[16] Biancolini M, Brutti C, Pennestri E, Valentini P. Dynamic, mechanical efficiency, and fatigue analysis of the double cardan homokinetic joint. Int J Veh Des 2003;32(3–4):231–49.

[17] Yang Z-X. Oscillation in electric power steering test torque due to universal joint angle and control strategy. J Dyn Syst Meas Control 2013;135(5).

[18] Abe M. Vehicle handling dynamics: Theory and application. Butterworth-Heinemann; 2015.

[19] Zheng H, Zhou J, Li B. Design of adjustable road feeling performance for steering-by-wire system. SAE Int J Veh Dyn, Stab, NVH 2018;2(2):121–34.

Jung Hyun Choi (S'19) received the B.S. and M.S. degrees in mechanical engineering from Yeungnam University, Korea, in 2010, and 2013, respectively, and the Ph.D. degree in the Department of Robotics Engineering of Daegu Gyeongbuk Institute of Science and Technology (DGIST), Daegu, Korea, in 2021.

From 2013 to 2016, he was a Researcher at the IoT and Robotics Research Division of DGIST. Since 2021, he has been an postdoctoral researcher at the DGIST, Daegu, Korea. His research interests include the development of mobile robot control algorithms, mechanical design, motion control.

Kanghyun Nam (S'10–M'12) received the B.S. degree in mechanical engineering from Kyungpook National University, Daegu, Republic of Korea, in 2007, the M.S.degree in mechanical engineering from Korea Advanced Institute of Science and Technology, Daejeon, Republic of Korea, in 2009, and the Ph.D.degree in electrical engineering from The University of Tokyo, Tokyo, Japan, 2012.

From 2012 to 2015, he was a Senior Engineer with Samsung Electronics Co., Ltd., Gyeonggi-do, Republic of Korea. Since 2015, he has been an Assistant Professor with the School of Mechanical Engineering, Yeungnam University, Gyeongbuk, Republic of Korea. His research interests include motion control, vehicle dynamics and control, electric vehicles.

Prof. Nam is a member of the Korean Society of Automotive Engineers. He received the Best Paper Award from the IEEE T RANSACTION ON I NDUSTRIAL E LECTRONICS in 2014.

Sehoon Oh (S'05–M'06–SM'16) received the B.S., M.S., and Ph.D. degrees in electrical engineering from The University of Tokyo, Tokyo, Japan, in 1998, 2000, and 2005, respectively.

He was a research associate at The University of Tokyo until 2012, a Visiting Researcher at the University of Texas at Austin from 2010 to 2011, a Senior Researcher at the Samsung Heavy Industries, and a Research Professor at Sogang University. He is currently an Assistant Professor at the DGIST, Daegu, South Korea. His research interests include the development of force control for human-friendly motion control algorithms and assistive/exercise devices for people.

Dr. Oh received the Best Transactions Paper Award from the IEEE Transactions on Industrial Electronics in 2013.